Microporous and Mesoporous Materials 255 (2018) 69–75

Contents lists available at ScienceDirect

Microporous and Mesoporous Materials

journal homepage: www.elsevier.com/locate/micromeso

Synthesis of Al_2O_3/carbon composites from wastewater as superior adsorbents for Pb(II) and Cd(II) removal

Hang Chen [a], Jianmin Luo [a], Xiao Wang [a], Xiaoyu Liang [a], Yunlong Zhao [a], Chao Yang [a], Murzabek Ispolovich Baikenov [b], Xintai Su [a, *]

[a] Ministry Key Laboratory of Oil and Gas Fine Chemicals, College of Chemistry and Chemical Engineering, Xinjiang University, Urumqi 830046, China
[b] The Department of Chemistry Technology and Oil, Buketov Karaganda State University, Karaganda 100028, Kazakhstan

ARTICLE INFO

Article history:
Received 2 March 2017
Received in revised form
5 June 2017
Accepted 15 July 2017
Available online 15 July 2017

Keywords:
Al_2O_3/carbon composite
Adsorption
Heavy metal ions
Water treatment
Recycle

ABSTRACT

Al_2O_3/carbon (Al_2O_3/C) composites obtained from the alkaline wastewater of oil refinery and acid wastewater of aluminum anodizing factory have been studied with the principle of "using waste to treat waste". The process includes these steps: (1) acid-alkali neutralization, (2) evaporation, (3) calcination, (4) washing and drying. The Al_2O_3/C composites prepared by calcinating the precursors under Ar atmosphere are used as high-capacity adsorbents for removal of Pb(II) and Cd(II) from aqueous solutions. For Pb(II), the adsorptive behavior satisfies the Langmuir assumptions and the maximum adsorption capacity reaches to 709.2 mg g^{-1}. For Cd (II), the adsorptive behavior satisfies the Freundlich assumptions and the equilibrium adsorption capacity is up to 1299.4 mg g^{-1}. For single adsorption of Pb(II) and Cd(II), the adsorption kinetics follows Pseudo-second-order model well. This route shows a possible way of reducing emissions to the environment, recovering resource as a valuable material, and providing a novel strategy for wastewater treatment.

1. Introduction

Nowadays, with the rapid development of industry, more and more environmental pollution problems have been brought into focus. Although people get immense economic benefit from it, it also inevitably produces lots of pollutants in air, soil, especially in water. Water pollution has put agriculture, environment, and human survival into a dangerous situation [1–4]. Accordingly, water treatment plays an increasingly important role in human daily life. Meanwhile lots of methods have been developed and practiced for water treatment in recent a few decades, which includes filtration, screening, micro-filtration, centrifugation, evaporation, ion exchange, adsorption, photocatalysis, etc [5–7].

Alkaline wastewater is generated from petroleum refinery, which contains plenty of aliphatic and aromatic organic pollutants. These contaminants pose serious toxic hazards to environment. What's more, methods for treating those effluents such as coagulation [8], chemical oxidation [9], photocatalytic degradation [10], and biological techniques [11] have also been reported. Generally, these methods involve transfer of pollutants from one medium to another; therefore, another step is asked for the elimination of organic compounds, which makes total treatment process become more complex and expensive. Acid wastewater is another major pollutant in aluminum anodizing industry. Anodizing is an electrochemical process to form an oxide film over aluminum layer, which can provide hardness and corrosion resistance to aluminum products. This process will consume large amount of electrolytes (sulphuric acid, phosphoric acid, hydrochloric acid, etc. [12]) and generate large quantities of wastewater, which contains large amounts of aluminum ion (Al^{3+}) and hydrogen ion (H^+). At present, the most conventional and popular treatment of waste acid is neutralization by mixing them with excessive lime milk in area of Xinjiang, China. However, the whole process needs to cost large amount of lime milk and produces a great deal of waste residue which is hard to be recovered and recycled. Therefore, it's highly essential to adopt an effective way to control these wastewater.

"Using waste to treat waste" [13–16] is a new trend for pollutant control. In the present study, an innovative method is proposed to treat two kinds of wastewater according this principle. With a facile neutralization process, two types of wastewater are mixed and dried to produce a precursor containing Al^{3+}, organic matter and sodium sulfate (Na_2SO_4). Subsequently, the as-prepared precursors

* Corresponding author.
E-mail address: suxintai827@163.com (X. Su).

http://dx.doi.org/10.1016/j.micromeso.2017.07.023
1387-1811/

are calcinated under Ar atmosphere at high temperature to obtain Al_2O_3/C composites. During the calcination process, the abundant organic matters can serve as a carbon source, and Na_2SO_4 can be directly used as a sacrificial template according to the melting salt method [17–19].

Heavy metals are basically recognized to be a threat toward ecosystems and humans because of their high potential toxicity. Besides, they can not be biologically decomposed into harmless materials and, to matters worse, are accumulated in the organisms [20]. Until now, adsorption is one of the most effective technologies of advanced wastewater treatment which is employed to reduce hazardous organic/inorganic pollutants present in the effluent by industries [21]. What's more, synthesizing alumina-coated carbon materials as an adsorbent for heavy metal ions removal has already been researched by some groups [22]. Thus, in the present work, two heavy metal ions (Pb(II) and Cd(II)) are induced as the model pollutants to study adsorption performance of Al_2O_3/C composites. The work have been completed in the present research including: i) Determine the optimal calcinating temperature. ii) Characterize the adsorbents with XRD, SEM equipped with an EDX analyzer, BET, and Raman. iii) Examine Pb(II) and Cd(II) sorption isotherms and kinetics onto Al_2O_3/C composites. This versatile method exhibits a promising application in water treatment, and provide a recyclable strategy to control waste by waste.

2. Materials and methods

2.1. Materials

Alkaline and acid wastewater were obtained separately from oil refinery of Dushanzi Petrochemical Corporation (Xinjiang, China) and aluminum anodizing factory of Joinworld Co., Ltd. (Xinjiang, China). The analysis of wastewaters were illustrated in Table 1. Sodium hydroxide (NaOH) was purchased from Tianjin Baishi Chemical Co., Ltd and was of analytical grade. All aqueous solutions were prepared with deionized water.

2.2. Preparation of Al_2O_3/C composites

In a typical synthesis, 150 mL of alkaline wastewater was filtered into a conical flask, and 200 mL of acid wastewater was added into conical flask. Then, 0.01 mol L^{-1} of NaOH solution was added to the mixture drop by drop with shaking to adjust pH value to 9. At the same time, the mixture appeared a precipitation, and the precipitation did not dissolve within 5 s. The obtained mixture was transferred to a watch glass, and dried at 80 °C in air. After drying, mixture was grounded in a mortar to form a fine powder. Subsequently, the powder was calcinated at a target temperature (550, 600, and 650 °C: noted as S-550, S-600, and S-650) with a heating rate of 10 °C·min^{-1} and kept at that temperature for 3 h under argon atmosphere. After cooling down, the products were washed with deionized water and dehydrated in a vacuum freeze dryer. Finally, the Al_2O_3/C composites were prepared by this method.

2.3. Characterizations

The morphology and chemical compositions of samples were characterized by a field-emission scanning electron microscopy (FESEM) in a Hitachi SU8010 equipped with a link energy-dispersive spectroscopy (EDS) analytical microprobe. The crystal structure of the samples were determined by X-ray diffraction (XRD, BRUKER D8 with Cu Kα radiation (λ = 1.54178 Å)). The Brunauer-Emmett-Teller (BET) specific surface area and pore volume were measured on a nitrogen adsorption apparatus (JW-BK, China) at 77 K. Desorption isotherms were used to calculate the pore size distributions using the Barret-Joyner-Halender method. Raman spectra were measured by Bluker Senterra with 532 nm wavelength laser source.

2.4. Batch adsorption test

To investigate removal of samples (S-550, S-600, S-650) prepared with different temperatures, a series of adsorption experiments were conducted using lead nitrate ($Pb(NO)_2$) and Cadmium nitrate ($Cd(NO)_2$) as a simulation of pollutants in water. 30 mg of Al_2O_3/C composites were well-dispersed into 50 mL of Pb(II) and Cd(II) solutions (100 mg/L) separately with a constant stirring in the dark. Then, samples were drawn from solution at predetermined time intervals, and centrifuged to measure the Pb(II)/Cd(II) removal via an atomic absorption spectroscopy (Hitachi, Z-2000, Japan). The metal ions removal efficiency R (%) were calculated by Equation (1):

$$R = [(C_0 - C_t)/C_0\ ]^* 100 \quad (1)$$

here C_0 (mg L^{-1}) is the initial metal ion concentration and C_t (mg L^{-1}) is residual metal ion concentration in solution at any time t (min).

To estimate adsorption capacity, 50 mg of S-600 was added to 100 mL of Pb(II) and Cd(II) solutions respectively. These solutions, with different concentrations (100–1000 mg L^{-1}), were stirred in the dark at equilibrium time. Then the amounts of metal ion adsorbed on Al_2O_3/C composites, q_t (mg g^{-1}) were calculated by the following Equation (2):

$$q_t = (C_0 - C_t)\ V/m \quad (2)$$

here q_t (mg g^{-1}) was the adsorption capacity at any time t (min). V (L) was the volume of the solution, and m (g) is the mass of adsorbents.

3. Results and discussion

3.1. Characterizations of Al_2O_3/C composites

The XRD patterns of samples were showed in Fig. 1. In figure, samples exhibited complex crystal phase and peak position, because of complex composition of the two different wastewater. Also, some impure peaks appeared, and the major peaks could be identified as γ- Al_2O_3 and carbon [23], respectively, in Fig. 1. In order to figure out the element component of samples, the energy dispersive spectrometer (EDS) exhibited in Fig. 2(e–f) confirmed that the as-prepared products were mainly composed of C, O, and Al elements. Thus, it could be concluded from XRD and EDS images that Al_2O_3/C composites had been successfully synthesized. SEM images of as-prepared products were showed in Fig. 2(a–c). From Fig. 2(a–c), it could be seen that the morphologies of as-prepared products were different. S-600 was some porous thin sheets, while S-550 and S-650 were small nanoparticles. Combining SEM

Table 1
Chemical composition of alkaline wastewater and acid wastewater.

Alkaline wastewater	Contents (mg L^{-1})	Acid wastewater	Contents (mg L^{-1})
pH	13.4	pH	0.3
COD	50000–60000	Al	6329
Phenols	600	SO_4^{2-}	13269
Ammonia	3557	Fe	31
Sulphides	7500	Mg	52
TDS	20000	Ca	511

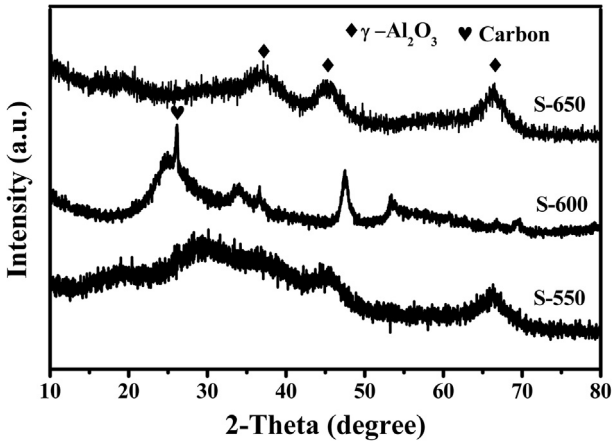

Fig. 1. The XRD patterns of samples calcinated at different temperature.

with EDS images, it could be concluded that the morphologies of products had a close connection with the content of carbon.

The nitrogen adsorption-desorption isotherms and pore size distribution of samples were showed in Fig. 3. The BET surface area and average pore diameter of samples were listed in Table 2. The as-prepared samples were of high surface areas and good porous properties, which are superior to many similar materials [24–26]. It turns out that this composites have a wide application in catalysis and adsorption field.

Raman spectroscopy is a widely used tool for the characterization of carbon products. Fig. 4 presented that Al_2O_3/C composites existed disorder and amorphous carbon and carbon compound resulted from the degree of the carbonization. Raman bands of carbonized samples appeared at the positions of approximately 1344 and 1590 cm^{-1}, corresponding to the in-plane vibrations of sp^2-bonded carbon with structural imperfections (D band) and to the in-plane vibrations of the sp^2-bonded crystalline carbon (G band), respectively [27–30]. S-600 was of highest intensity of D and G band, indicating that the framework of carbon membrane had more defects and became a more graphitized carbon wall at 600 °C [31]. The Blue shift of Raman peak of S-600 might be due to the change in the size of the samples and the band gap [14]. What's more, changes in the peak position may also be related to interatomic forces and equilibrium positions of the lattice change [32]. The above analysis might explain why S-600 has a higher adsorption performance than S-550 and S-650.

3.2. Adsorptive properties for Pb(II) and Cd(II)

To further investigate adsorption performance of samples for removing heavy metal ions in water treatment, Pb(II) and Cd(II)

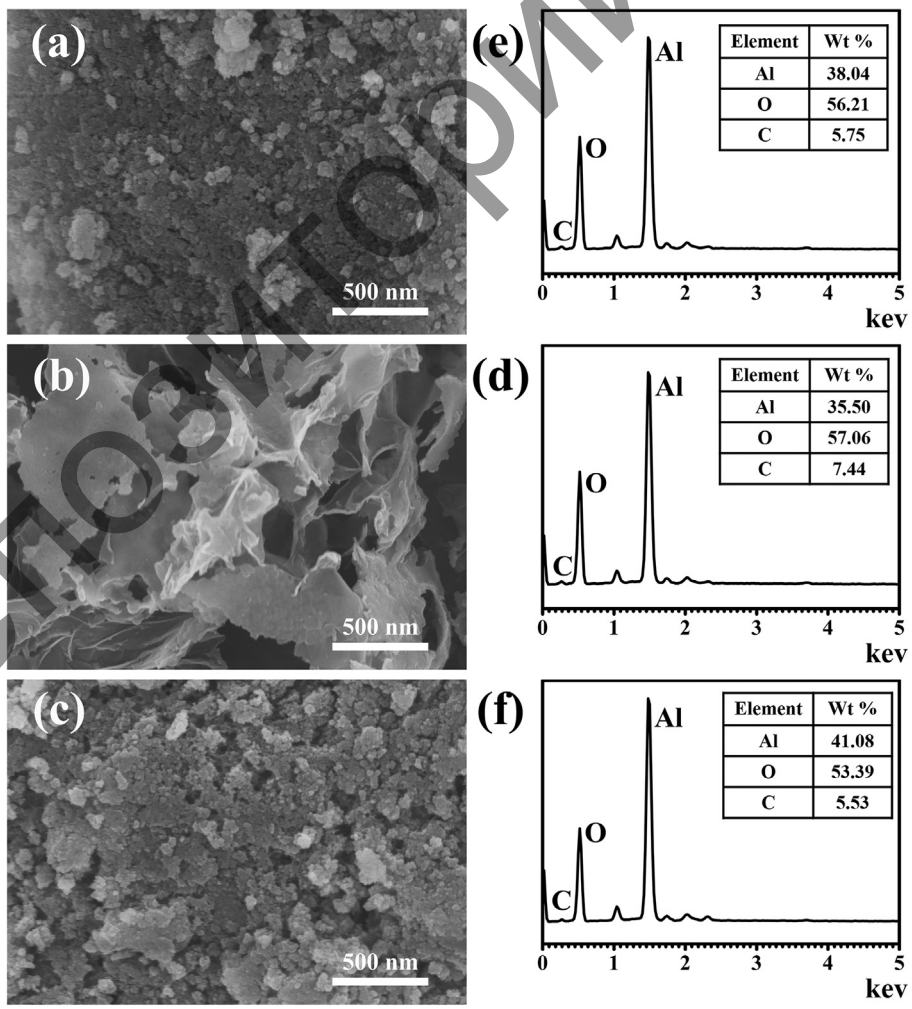

Fig. 2. SEM micrographs and the corresponding EDS analysis of (a, e) S-550, (b, d) S-600 and (c, f) S-650.

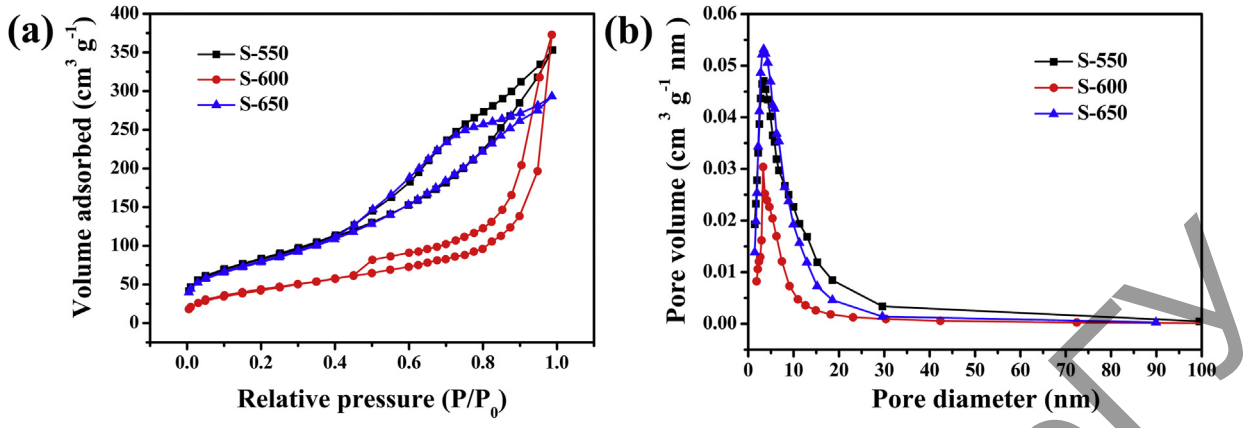

Fig. 3. (a) Nitrogen adsorption-desorption isotherms and (b) the corresponding pore size distributions curves for as-prepared Al_2O_3/C composites.

Table 2
BET characteristics of Al_2O_3/C produced at 550/600/650 °C.

Adsorbents	BET surface area (m^2 g^{-1})	Pore volume (cm^3 g^{-1})	Average pore (nm)
S-550	299.56	0.55	14.70
S-600	358.59	0.21	6.513
S-650	289.06	0.45	14.70

were introduced to explore advantage of adsorbents, respectively. In the present study, remove efficiency of heavy metal ions was researched to compare the adsorptive properties of S-550, S-600, and S-650. Then, the sample with highest removal was selected to research the adsorption isotherms and adsorption kinetics.

3.2.1. Removal

Fig. 5 showed the removal of Pb(II) and Cd(II) on three different temperatures (550, 600, and 650 °C), which had reached an equilibrium within 2.5 h. S-600 exhibited the highest removal among three samples, and approximately 83% of Pb(II) and 78% of Cd(II) were removed within 25 min, respectively. After 250 min, approximately 97% of Pb(II) and 90% of Cd(II) were removed by S-600. The higher removal of Pb(II) might be attributed to the various active sites on adsorbents having different affinities to Pb(II) and Cd(II). The great adsorption performance of S-600 might result from its higher carbon content, special morphologies, and big surface area. The measured data could be further applied for the investigation of the adsorption kinetics of Pb(II) and Cd(II).

3.2.2. Adsorption isotherms

The adsorption capacities and removal of Pb(II) and Cd(II) on S-600 were depicted in Fig. 6. Obviously, it could be observed that the adsorption capacities of adsorbents increased with increasing C_0 at first, for both Pb(II) and Cd(II), and then reached an equilibrium. The remove efficiencies still were approximately 30% and 65%, for Pb(II) and Cd(II) respectively, when initial concentration of Pb(II) and Cd(II) increased to 1000 mg L^{-1}.

The amount of heavy metal ions adsorbed at equilibrium q_e (mg g^{-1}) had been calculated from the following Equation (3):

$$q_e = (C_0 - C_e)v/m \quad (3)$$

here C_0 (mg L^{-1}) is the initial dye concentration, C_e (mg L^{-1}) is the equilibrium concentration of dye solution, v (L) is the volume of dye solution, and m (g) is the mass of adsorbent.

The adsorption process could be expressed by two isotherm equations, namely, the Langmuir and the Freundlich equations, which were represented by the following Equation (4) and Equation (5), respectively:

$$C_e/q_e = 1/(K_L\, q_m) + C_e/q_m \quad (4)$$

$$q_e = K_f\, C_e^{1/n} \quad (5)$$

here q_m (mg g^{-1}) and K_L (L mg^{-1}) are Langmuir isotherm coefficients. The value of q_m represents the maximum adsorption capacity. K_f and n are Freundlich constants.

The linear plots of the Langmuir model and Freundlich model of the adsorption for Pb(II) and Cd(II) were showed in Fig. 7. The adsorption isotherm parameters of both models were listed in Table 3. For Pb(II), It was found that the adsorption data were well fitted with Langmuir model with correlation coefficients (R^2 = 0.9766), which indicated that the adsorption of Pb(II) on S-600 was a monolayer chemical sorption process and the maximum adsorption capacity q_m was 709.2 mg g^{-1}. For Cd(II), the data showed satisfactory compliance with Freundlich model with high correlation coefficients (R^2 = 0.9856), better than Langmuir (R^2 = 0.9096). The equilibrium adsorption capacity reached to 1299.4 mg g^{-1}. Table 4 exhibited the comparison of Pb(II) and Cd(II) adsorption capacity of various adsorbents in the previous study. It could be seen that the prepared Al_2O_3/C composites is of much higher removal performance of heavy metal ions than many other adsorbents reported in the literature.

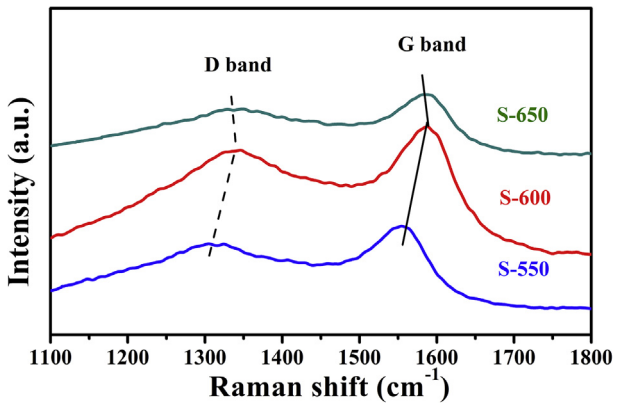

Fig. 4. Raman spectra of Al_2O_3/C composites calcinated at different temperature.

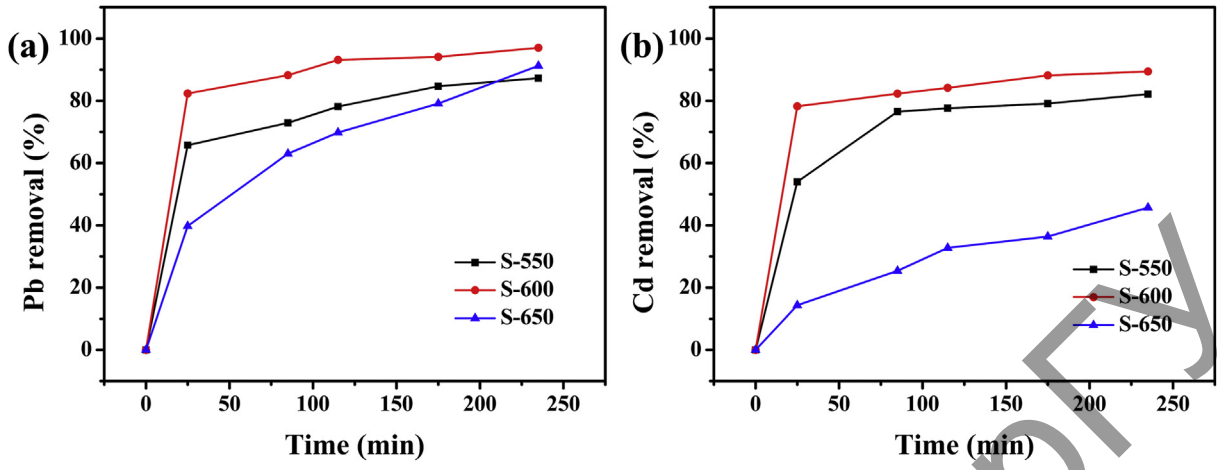

Fig. 5. The removal of heavy metal ions (100 mg L^{-1}, 50 mL) on S-550, S-600, and S-650: (a) Pb(II) and (b) Cd(II).

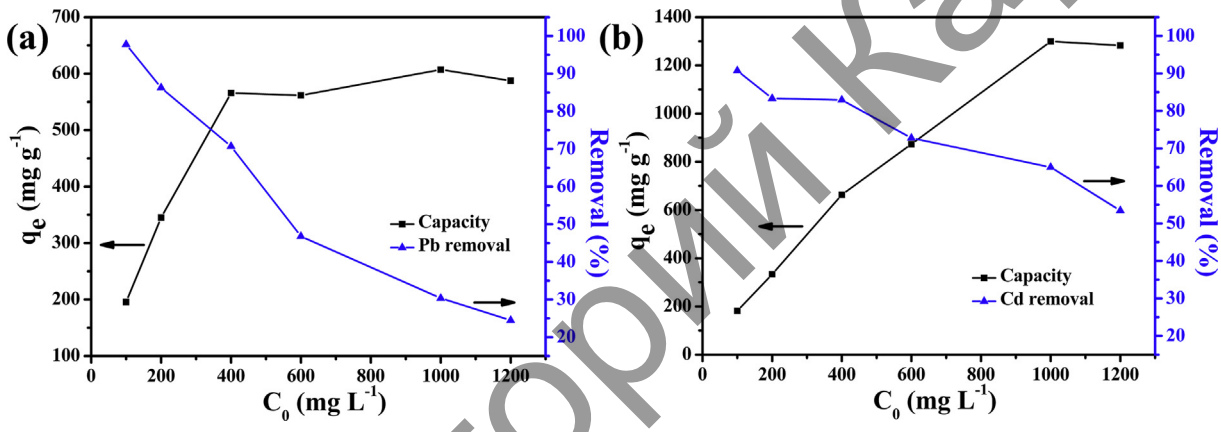

Fig. 6. Adsorption isotherm and removal of heavy metal ions as a function of initial concentration: (a) Pb(II) and (b) Cd(II).

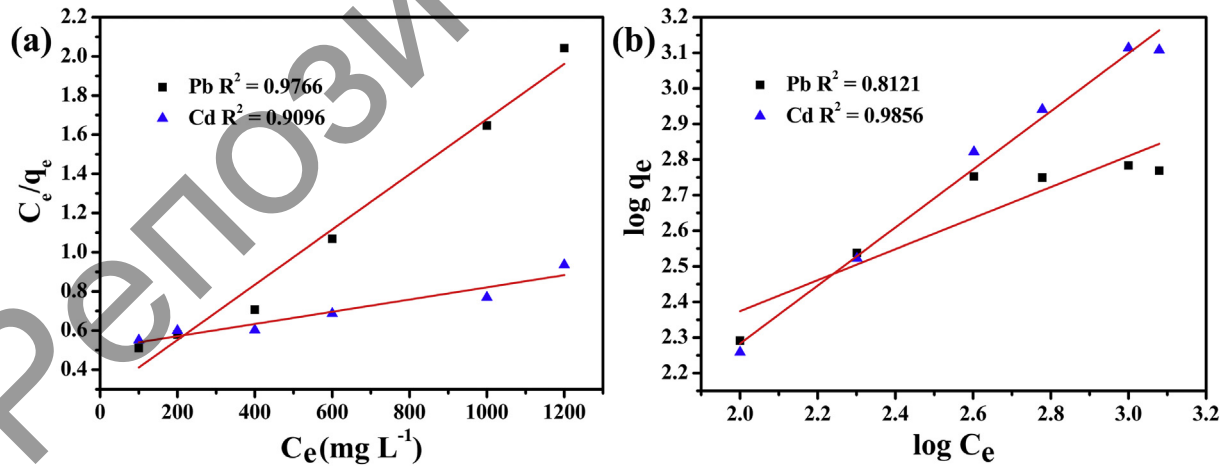

Fig. 7. (a) The linear Langmuir and (b) the Freundlich adsorption isotherms for Pb(II) and Cd(II) adsorption by S-600.

3.2.3. Adsorption kinetics

The kinetics of heavy metal ions adsorption on S-600 was further investigated. The pseudo-first-order kinetic model and pseudo-second-order kinetic models were used to describe this adsorption process, respectively.

The pseudo-first-order kinetic model could be expressed with Equation (6):

$$\log (q_e - q_t) = \log q_e - K_1\, t/2.303 \quad (6)$$

Table 3
Adsorption isotherm parameter of S-600.

Metal ions	Langmuir isotherm model			Freundlich isotherm model		
	q_m (mg g^{-1})	K_L (L mg^{-1})	R^2	K_f (mg g-1) (mg-1 L)1/n	n	R^2
Pb(II)	709.2	5.21×10^{-3}	0.9766	31.83	2.30	0.8121
Cd(II)	3201.3	6.13×10^{-4}	0.9096	4.48	1.23	0.9856

Table 4
Comparison of Pb (II) or Cd(II) adsorption capacity of various adsorbents.

Adsorbents	Adsorbates	Adsorption capacity (mg g^{-1})	References
Al_2O_3/C composites	Pb(II)	709.2	this study
Al_2O_3-supported iron oxide	Pb(II)	29.01	[33]
Al_2O_3	Pb(II)	17.5	[34]
sawdust of pinus sylvestris	Pb(II)	22.22	[35]
titanate nanotubes	Pb(II)	520.83	[36]
Ca-Montmorillonite	Pb(II)	13.650	[37]
water hyacinth biochar	Pb(II)	168	[38]
grapheme oxide/cellulose	Pb(II)	107.9	[39]
Activated alumina	Pb(II)	13.11	[41]
Al_2O_3/C composites	Cd(II)	1299.4	this study
Al_2O_3	Cd(II)	17.7	[34]
Mg-Al-CO_3-LDH	Cd(II)	61.4–70.2	[40]
sawdust of pinus sylvestris	Cd(II)	19.08	[35]
titanate nanotubes	Cd(II)	238.61	[36]
Ca-Montmorillonite	Cd(II)	30.675	[37]
water hyacinth biochar	Cd(II)	77.5	[38]
grapheme oxide/cellulose	Cd (II)	26.8	[39]
Activated alumina	Cd (II)	8.24	[41]

here q_e and q_t (mg g^{-1}) are the adsorption capacities at equilibrium and at time t (min), respectively. K_1 (min^{-1}) is the rate constant for pseudo-first-order adsorption. The values of rate constant can be obtained from the slope of the plot of $lg(q_e\text{-}q_t)$ versus t.

The pseudo-second-order kinetic model could be expressed with Equation (7):

$$t/q_t = 1/(K_2\, q_e^2) + t/q_e \quad (7)$$

here K_2 (g mg^{-1} min^{-1}) is the rate constant of the pseudo-second-order adsorption. K_2 and q_e are determined from the intercept and slope of the plot t/q_t versus t.

Table 5
Adsorption parameter of kinetics for the adsorption of Pb(II) and Cd(II) onto S-600.

Metal ions	Pseudo-first-order			Pseudo-second-order		
	q_e (mg g^{-1})	K_1 (min^{-1})	R^2	q_e (mg g-1)	K_2 (g mg^{-1} min^{-1})	R^2
Pb(II)	31.5	0.011	0.9041	161.6	0.001	0.9990
Cd(II)	35.9	0.005	0.9775	150.2	0.001	0.9982

The kinetic parameters and the correlation coefficients (R^2) were obtained and showed in Fig. 8 and Table 5. The lower correlation coefficients suggested that the pseudo-first-order could not describe the adsorption process correctly. On the contrary, the pseudo-second-order model provided excellent correlation coefficients ($R^2 > 0.99$) of Pb(II) and Cd(II). Hence it could be inferred that the adsorption of Pb(II) and Cd(II) onto S-600 perfectly followed the pseudo-second-order kinetic model, implying that the rate-controlling step might be chemisorptions [42,43] involving valence forces through sharing or exchange of electrons [44].

4. Conclusion

In summary, based on the thoughts of "using waste to treat waste" and "waste resource recovery", the Al_2O_3/C composites are successfully fabricated from two wastewater. Such way not only eliminates two refractory contaminants without adding additional agents, but also obtains an adsorbent with excellent performance. The removal of Pb(II) and Cd(II) on Al_2O_3/C composites can be as high as 97% and 90%, respectively, when the calcinating temperature is 600 °C. The adsorption behavior of Pb(II) and Cd(II) on S-600 suggest the adsorption isotherms are well fitted with the Langmuir model and Freundlich model, respectively. For Pb(II), the maximum adsorption capacity of S-600 is up to 709.2 mg g^{-1}. For Cd(II), the equilibrium adsorption capacity reaches to 1299.4 mg g^{-1}. The

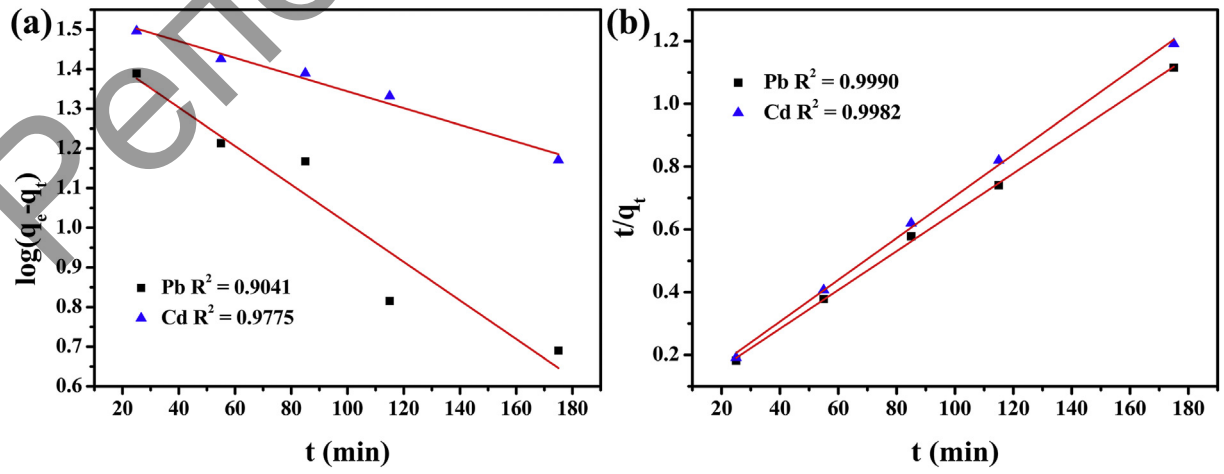

Fig. 8. Plots of kinetic models for the adsorption of Pb(II) and Cd(II) on S-600: (a) pseudo-first-order kinetics, (b) pseudo-second-order kinetics.

superior performance for heavy metal ions can be ascribed to their special structures and high surface area that can expose more adsorption sites. Kinetics of adsorption on S-600 is found to follow the pseudo second-order rate equation for both ions. This study has shown a low-cost, versatile, and recycling route for water treatment, and indicates the as-prepared Al_2O_3/C composites can be used as potential candidate for heavy metal ions removal.

Acknowledgments

This work was supported by the National Natural Science Foundation of China (21566037, U1503391 and 51174174).

References

[1] E.D. Ongley, Control of Water Pollution from Agriculture, Food & Agriculture Org., Burlington, 1996.
[2] C.J. Vörösmarty, P.B. Mcintyre, M.O. Gessner, D. Dudgeon, A. Prusevich, P. Green, S. Glidden, S.E. Bunn, C.A. Sullivan, C.R. Liermann, Nature 467 (2010) 555–561.
[3] Y. Lu, S. Shuai, R. Wang, Z. Liu, M. Jing, A.J. Sweetman, A. Jenkins, R.C. Ferrier, L. Hong, L. Wei, Environ. Int. 77 (2015) 5–15.
[4] R.P. Schwarzenbach, T. Egli, T.B. Hofstetter, U.V. Gunten, B. Wehrli, Annu. Rev. Env. Resour. 35 (2010) 109–136.
[5] V.K. Gupta, I. Ali, T.A. Saleh, A. Nayak, S. Agarwal, RSC Adv. 2 (2012) 6380–6388.
[6] I. Ali, Chem. Rev. 112 (2012) 5073–5091.
[7] N.C. Meng, J. Bo, C.W.K. Chow, C. Saint, Water Res. 44 (2010) 2997–3027.
[8] M.H. El-Naas, S. Al-Zuhair, A. Al-Lobaney, S. Makhlouf, J. Environ. Manage 91 (2009) 180–185.
[9] O. Abdelwahab, N.K. Amin, E.S. Elashtoukhy, J. Hazard. Mater 163 (2009) 711–716.
[10] J. Saien, H. Nejati, J. Hazard. Mater 148 (2007) 491–495.
[11] D.E. Mazzeo, C.E. Levy, A.D.F. De, M.A. Marinmorales, Sci. Total Environ. 408 (2010) 4334–4340.
[12] S.H. Lin, C.L. Mu, J. Hazard. Mater 60 (1998) 247–257.
[13] Z.J. Hu, Y. Xiao, D.H. Zhao, Y.L. Shen, H.W. Gao, J. Hazard. Mater 175 (2010) 179–186.
[14] X. Liang, Y. Lu, Z. Li, C. Yang, C. Niu, X. Su, Microporous Mesoporous Mater 241 (2017) 107–114.
[15] S. Dawood, T.K. Sen, Water Res. 46 (2012) 1933–1946.
[16] E.S.Z. El-Ashtoukhy, N.K. Amin, O. Abdelwahab, Desalination 223 (2008) 162–173.
[17] G. Wu, X. Liang, H. Zhang, L. Zhang, F. Yue, J. Wang, X. Su, Catal. Commun. (2016) 63–67.
[18] B. Yan, J. Zhou, X. Liang, K. Song, X. Su, Appl. Surf. Sci. 392 (2017) 889–896.
[19] B. Jang, M. Park, O.B. Chae, S. Park, Y. Kim, S.M. Oh, Y. Piao, T. Hyeon, J. Am. Chem. Soc. 134 (2012) 15010.
[20] F. Ribeyre, C. Amiard-Triquet, A. Boudou, J.C. Amiard, Ecotoxicol. Environ. Saf. 32 (1995) 1–11.
[21] M.T. Yagub, T.K. Sen, S. Afroze, H.M. Ang, Adv. Colloid Interface Sci. 209 (2014) 172–184.
[22] V.K. Gupta, S. Agarwal, T.A. Saleh, J. Hazard. Mater 185 (2011) 17–23.
[23] S. Wang, C. Zhang, G. Sun, Y. Yuan, L. Chen, X. Xiang, Q. Ding, B. Chen, Z. Li, X. Zu, J. Lumin 153 (2014) 393–400.
[24] Y.I. Tarasevich, G.M. Klimova, Appl. Clay Sci. 19 (2001) 95–101.
[25] A. Afkhami, M. Saber-Tehrani, H. Bagheri, J. Hazard. Mater 181 (2010) 836–844.
[26] X. Liu, C. Niu, X. Zhen, J. Wang, X. Su, J. Colloid Interface Sci. 452 (2015) 116–125.
[27] P.D. Green, C.A. Johnson, K.M. Thomas, Fuel 62 (1983) 1013–1023.
[28] C.A. Johnson, J.W. Patrick, K.M. Thomas, Fuel 65 (1986) 1284–1290.
[29] G. Katagiri, H. Ishida, A. Ishitani, Carbon 26 (1988) 565–571.
[30] M. Nakamizo, H. Honda, M. Inagaki, Carbon 16 (1978) 281–283.
[31] S. Tanaka, T. Yasuda, Y. Katayama, Y. Miyake, J. Membr. Sci. 379 (2011) 52–59.
[32] L. Li, B. Suen, F. Talke, IEEE T. Magn. 51 (2015) 1.
[33] Y.H. Huang, C.L. Hsueh, C.P. Huang, L.C. Su, C.Y. Chen, Sep. Purif. Technol. 55 (2007) 23–29.
[34] J. Yin, Z. Jiang, G. Chang, B. Hu, Anal. Chim. Acta 540 (2005) 333–339.
[35] V.C. Taty-Costodes, H. Fauduet, C. Porte, A. Delacroix, J. Hazard. Mater 105 (2003) 121–142.
[36] L. Xiong, C. Chen, Q. Chen, J. Ni, J. Hazard. Mater 189 (2011) 741–748.
[37] Y. Li, J. Wang, X. Wang, J. Wang, Ind. Eng. Chem. Res. 51 (2012) 6520–6528.
[38] Y. Ding, Y. Liu, S. Liu, Z. Li, X. Tan, X. Huang, G. Zeng, Y. Zhou, B. Zheng, X. Cai, RSC Adv. 6 (2016) 8.
[39] R. Sitko, M. Musielak, B. Zawisza, E. Talik, A. Gągor, RSC Adv. 6 (2016) 96595–96605.
[40] R.R. Shan, L.G. Yan, K. Yang, Y.F. Hao, B. Du, J. Hazard. Mater 299 (2015) 42–49.
[41] Y.J.O. Asencios, M.R. Sun-Kou, Appl. Surf. Sci. 258 (2012) 10002–10011.
[42] T.K. Sen, M.V. Sarzali, Chem. Eng. J. 142 (2008) 256–262.
[43] D.G. Strawn, A.M. Scheidegger, D.L. Sparks, Environ. Sci. Technol. 32 (1998) 2596–2601.
[44] Y.S. Ho, G. Mckay, Water Res. 34 (2000) 735–742.